# Physical, chemical and electrical study of $0.1Li_2O$-$0.4MO$-$0.5P_2O_5$ oxide glasses M (Zn, Pb, Cu, Ba, Cd).

*Lahbib* ABBAS[1*], *Lahcen* BIH[2], *Abdelaziz* AIT SIDI MOU[1] and *Zahra* RAMZI[3]

[1]Chemistry-Physics, Electrochemistry, and Environment Team, Faculty of Science and Technology, Moulay Ismail University, Er-Rachidia, Morocco;
[2]Laboratory of Engineering Sciences and Professions, National School of Arts and Crafts, Moulay Ismail University, Meknes, Morocco;
[3]Laboratory of Materials Physiochemistry and Environment (LPCME), Faculty of Sciences Semlalia, Cadi Ayyad University, Marrakech, Morocco.

**Abstract.** The study examines the physical and chemical properties of glassy and crystalline phosphate materials, emphasizing their structure characterized by ionic bonds linking chains of divalent metal cations to non-bridging oxygen atoms. It aims to determine the influence of specific divalent cations (Cu, Cd, Zn, Ba, Pb) on the attributes of glasses formulated with the composition $0.1Li_2O$-$0.4MO$-$0.5P_2O5$. We studied the physical and chemical properties of certain glasses, focusing on density, molar volume, glass transition temperature, and chemical durability. We also assessed their electrical characteristics and utilized IR spectroscopy for structural analysis. Key findings revealed that the glass molar volume increases with the atomic number of the divalent cation in the sequence: $V_m(Cu) < V_m(Zn) < V_m(Cd) < V_m(Ba) < V_m(Pb)$. Furthermore, the dissolution rate follows the order: $D_R(Zn) < D_R(Cd) < D_R(Ba) < D_R(Cu) < D_R(Pb)$. The glass transition temperature ($T_g$) increases in the order $T_g(Pb) < T_g(Cd) < T_g(Ba) < T_g(Zn) < T_g(Cu)$, indicating enhanced bond strength and compactness. Additionally, the divalent metal cation $M^{2+}$ affects the direct current conductivity ($\sigma_{dc}$) and activation energy ($E_a$), with only the $LiM_2(PO_3)_5$ phase forming as observed in the X-ray diffractograms of the crystalline glass related to the composition.

*Corresponding author: l.abbas@umi.ac.ma

## 1 Introduction

Phosphate glasses are promising due to their high thermal expansion coefficient and low melting temperature compared to silicate glasses, although their chemical durability in water limits their practical applications. Recent developments have expanded their use in specialised applications [1].
Phosphate glasses have various structures, ranging from tetrahedral cross-linked networks (vitreous $P_2O_5$) to polymeric metaphosphate chains, including "inverted" glasses, defined by the O/P ratio of their composition. The addition of a modifying oxide to $P_2O_5$ generates non-bridging oxygen (NBO) at the expense of bridging oxygen (BO).
Among the phosphate families, glassy metaphosphate has the least complex structure, composed of tetrahedra with bridging oxygen atoms forming chains and rings, connected by ionic bonds with various metal cations and non-bridging oxygen atoms. The chains and units are linked between various metal cations and non-bridging oxygen atoms by ionic bonds. Lithium ions are coordinated tetrahedrally [2]. This work aims to evaluate the impact of various divalent cations on the physical and chemical properties of $0.1Li_2O$-$0.4MO$-$0.5P_2O_5$ glasses with M (Cu, Cd, Zn, Ba, Pb), analysing how these cations modify the chemical environments of phosphorus due to their varied counterion potentials.
Recent studies of glass [3-7] have shown that the addition of MO with M (Cu, Cd, Zn, Ba, Pb) significantly increases corrosion resistance. This work examines the impact of bivalent cations on the physical and chemical properties of oxide glasses with a composition of $0.1Li_2O$-$0.4MO$-$0.5P_2O_5$, where M (Cu, Cd, Zn, Ba, Pb). The study includes the analysis of physical properties (density, molar volume, glass transition temperature) and chemical properties (chemical durability), as well as electrical properties, using IR spectroscopy to explore the structure of the glasses. The results show that the modification of the chemical environment of phosphorus, induced by cations, significantly influences the properties of glasses, particularly their chemical durability. Glasses with a composition of $0.1Li_2O$-$0.4MO$-$0.5P_2O_5$, which are particularly resistant to corrosion, show promise for glass electrolytes in applications such as renewable energy storage and electric vehicles.

### 2 Experimental procedures

Calcination involves mixing pure, fine-grained powders homogeneously to prepare glasses with a composition of $0.1Li_2O$-$0.4MO$-$0.5P_2O_5$, where M can be Cu, Cd, Zn, Ba or Pb, according to a specific reaction:

$$0.1Li_2O + 0.4MO + (NH_4)H_2PO_4 \leftrightarrow 0.1Li_2O\ 0.4MO\ 0.5P_2O_5 + NH_3 + 1.5H_2O \quad \text{Eq (1)}$$

where M = Cu, Cd, Zn, Ba, Pb.
Appropriate quantities of $Li_2CO_3$, $NH_4H_2PO_4$ and $BaCO_3$, $CdCO_3$, CuO, PbO or ZnO are ground in a mortar for 45 minutes in a dry environment. The mixture is placed in a platinum crucible and heated to 573 K/h in a furnace. Two heat treatments are carried out: the first at 533 K to decompose the ammonium phosphate, remove moisture and release $CO_2$, with calcination lasting 12 hours; the second at 1173 K for sintering, lasting 15 minutes.
Powder X-ray diffraction confirmed the amorphous state of all as-quenched glasses. Differential thermal analysis was performed at a heating rate of 383 K min-1 to determine the glass transition temperature ($T_g$). Density measurements at room temperature utilized Archimedes' method with xylene as the immersion liquid, and the molar volume ($V_m$) was calculated based on a defined formula:
$V_m = \sum y_i M_i / \rho$ (Eq. 1), where $y_i$ is the molar fraction of the oxide (i), ρ is the density and $M_i$ is its molecular weight.
The dissolution rate of the glasses in water was assessed by measuring the weight loss of samples immersed in deionized water at 363 K for 2 days. The samples were polished, cleaned with acetone, and placed in glass flasks with deionized water. Duplicate measurements were conducted for each glass, and the average dissolution rate was calculated, normalized to the glass surface area and corrosion time:

$D_R = \Delta W(g)/[A(cm^2) \times t(min)]$ (Eq. 2), where $A$ is the surface area ($cm^2$) of the sample and $t$ is the time (min) that the sample was immersed in the test solution at 363 K. The weight loss ($\Delta W$) is $W_i$ - $W_t$, where $W_i$ is the initial weight and $W_t$ is the weight of the same sample after a time t in solution at 363 K.

This dissolution rate ($D_R$) of each glass serves as a reference for assessing its chemical durability. Electrical measurements of the $0.1Li_2O$-$0.4MO$-$0.5P_2O_5$ (with M being Cu, Zn, Cd, Ba, Pb) glasses were conducted using an LCR-meter HP4284, in a frequency range of 20Hz to 1 MHz and a thermal range of 313-573K.
Devitrification by annealing of the glasses studied enabled their crystallisation kinetics and structure to be evaluated. The crystallised phases were identified using ICDD data. Successive annealing cycles of 12 hours at increasing temperatures in intervals of 293 K, above the glass transition temperature ($T_g$), were carried out.

## 3 Results and discussion

### 3. 1 Density and molar volume

The table shows the values for density (ρ), molar volume ($V_m$), crystalline molar volume ($V_c$), and the difference. $\Delta V = V_c - V_m$.

**Table. 1.** Data for the five glasses examined: composition, density ρ, experimental molar volumes $V_m$ and crystalline volumes $V_c$ and their difference ΔV.

| M | Ba | Pb | Cd | Zn | Cu |
|---|---|---|---|---|---|
| $\rho$ | 3.49 | 4.72 | 3.3 | 2.91 | 3.33 |
| $V_m$ ($cm^3$/mol) | 38.96 | 39.05 | 36.93 | 36.69 | 36.04 |
| $V_c$ ($cm^3$/mol) | 41.31 | 40.63 | 37.51 | 37.04 | 36.14 |
| $\Delta V$ | 2.35 | 1.58 | 0.58 | 0.35 | 0.1 |

The density of the glasses studied varies non-linearly, as shown in Table (1), and this variation can be explained by various factors:
When the divalent cation $Pb^{2+}$ is replaced by $Cu^{2+}$, the ionic radius decreases, as do the degree of negative charge and density. Thus, when the divalent cation $Pb^{2+}$ is replaced by the divalent cation $Ba^{2+}$, the ionic radius remains almost constant but the degree of negative charge decreases ($[Ba^{2+}] = [Xe]$; $[Pb^{2+}] = [Xe]4f^{14}\ 5d^{10}\ 6s^2$) and therefore the density decreases. Therefore, when the $Cu^{2+}$; ($Zn^{2+}$) or ($Cd^{2+}$) cation is replaced by the divalent $Ba^{2+}$ cation, the ionic radius decreases, as does the density. When the $Cu^{2+}$ or ($Zn^{2+}$) cation is replaced by the divalent $Cd^{2+}$ cation, the ionic radius decreases, as does the density. When the $Cu^{2+}$ cation is replaced by the divalent $Zn^{2+}$ cation, the ionic radii of $Cu^{2+}$ and $Zn^{2+}$ are very similar, whereas the effective nuclear charge of copper is higher than that of zinc, hence the density of copper is greater than that of zinc.
The experimental molar volume ($V_m$) of $0.1Li_2O$-$0.4MO$-$0.5P_2O_5$ glasses is derived from the molar mass and density. The crystalline molar volume ($V_c$), calculated by summing the molar volumes of the oxides, increases in the order $V_m$ (Cu glass) < $V_m$ (Zn glass) < $V_m$ (Cd glass) < $V_m$ (Ba glass) < $V_m$ (Pb glass), indicating that the molar mass of the cations influences $V_m$. The experimental values are systematically lower than the crystalline values, suggesting a more compact structure in glasses compared to their crystalline phases, and revealing that the incorporation of M ions (Cu, Cd, Zn, Ba, Pb) contracts the glass lattice and the arrangement of oxygen ions.

### 3. 2 Differential thermal analysis

Oxide glasses are considered oxygen polymers, with a glass transition temperature that increases with bond strength, cross-link density, and network compactness [8]. To determine the characteristic temperatures ($T_g$, $T_c$, $T_f$) of $0.1Li_2O$-$0.4MO$-$0.5P_2O_5$ glasses and study the effect of incorporating divalent metals M (Cu, Cd, Zn, Ba, Pb) into the $Li_2O$ - $P_2O_5$ glass framework, an analysis is performed using the ATD technique.
The ATD curve for $0.1Li_2O$-$0.4BaO$-$0.5P_2O_5$ glass, shown in Figure (1), is representative of the results obtained for other $0.1Li_2O$-$0.4MO$-$0.5P_2O_5$ glass compositions with M (Cu, Cd, Zn, Ba, Pb). These curves can be used to determine the transition ($T_g$), crystallisation ($T_c$) and melting ($T_f$) temperatures for each composition.

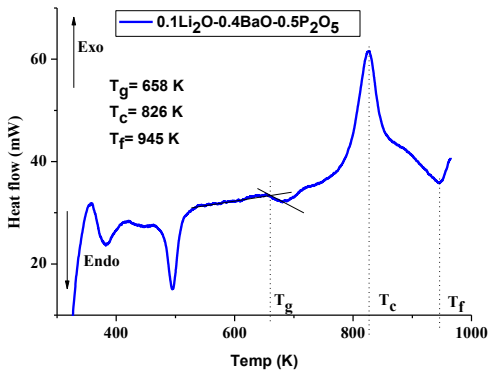


**Fig. 1.** ATD curve of glass with composition $0.1Li_2O$-$0.4BaO$-$0.5P_2$

**Table 2.** $T_g$ and $V_t$ of glasses with composition $0.1Li_2O$-$0.4MO$-$0.5P_2O_5$

| M | Pb | Cd | Ba | Zn | Cu |
|---|---|---|---|---|---|
| $T_g$ (K) | 721 | 744 | 757 | 782 | 882 |
| $V_t$ | 0.31 | 0.42 | 0.44 | 0.46 | 0.47 |

Table (2) shows the transition temperature $T_g$ and compactness $V_t$ for each glass composition.

In the study of five $0.1Li_2O$-$0.4MO$-$0.5P_2O_5$ glasses (where M represents Ba, Cd, Cu, Zn, Pb), it was observed that the glass transition temperature ($T_g$) increases with increasing compactness ($V_t$). Substituting a substance with high compactness for one with low compactness increases the bond energy, which leads to an increase in $T_g$. The incorporation of substances with stronger cross-links improves connectivity, making the glass network denser. Thus, high $V_t$ compactness is indicative of a more rigid network, where an increase in internal energy is required to achieve the mobility necessary for the glass transition, resulting in a decrease in $T_g$. Consequently, the order of increase in $T_g$ is $T_g$(Pb glass) < $T_g$(Cd glass) < $T_g$(Ba glass) < $T_g$(Zn glass) < $T_g$(Cu glass), reflecting an improvement in bond strength and bond density in the network. The slight increase in glass transition temperature ($T_g$) indicates a gradual change in structure. The incorporation of divalent cations M (Cu, Cd, Zn, Ba, Pb) into the $Li_2O$- $P_2O_5$ glass matrix shortens the phosphate chains by breaking the P-O-P bonds, thereby creating cross-linking ionic bonds. This phenomenon increases network connectivity, leading to a variation in $T_g$. Furthermore, the increase in the ionic radius of divalent cations, such

as lead, is associated with a decrease in $T_g$, suggesting that the nature of the bond influences this variation. The P-O-M bonds formed when one divalent ion is replaced by another show a change in the covalence of the M-O bonds. Thus, the order of covalence is discernible in Pb, Cd, Ba, Zn, and Cu glasses, indicating a compact and coherent network with increasing $T_g$.3. 3 Chemical durability

The dissolution rate $D_R$ of $0.1Li_2O$-$0.4MO$-$0.5P_2O_5$ glasses (where M = Cu, Cd, Zn, Ba, Pb) in distilled water at 363 K is shown in Table 3.

**Table 3**. Dissolution rate $D_R$ of $0.1Li_2O$-$0.4MO$-$0.5P_2O_5$ glasses

| M | Zn | Cd | Ba | Cu | Pb |
|---|---|---|---|---|---|
| $D_R$ (g $cm^{-2}$ $ml^{-1}$) × $10^5$ | 1.17 | 1.53 | 1.76 | 2.05 | 2.18 |

The results indicate that the dissolution rate of metaphosphate glasses follows the order $D_R$ (Zn glass) < $D_R$ (Cd glass) < $D_R$ (Ba glass) < $D_R$ (Cu glass) < $D_R$ (Pb glass), with zinc glass offering the best chemical durability and lead glass the lowest. A comparison between binary and ternary metaphosphate glasses shows that $D_R(0.5Li_2O$-$0.5P_2O_5)$ is significantly superior to $D_R(0.1Li_2O$-$0.4MO$-$0.5P_2O_5)$, regardless of the divalent cations. The increase in chemical durability is linked to doping with oxides, which improves the cross-links between phosphate units.

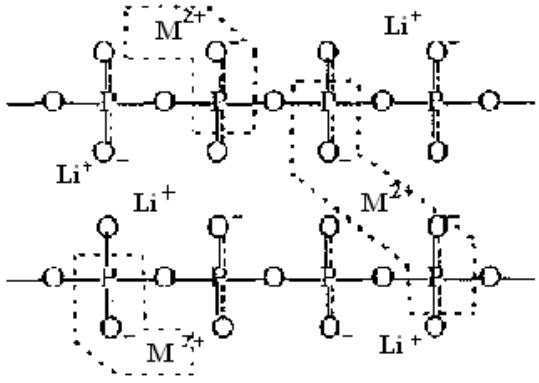


**Fig. 2.** Cross-link between divalent cations forming a chelate structure.

This type of metal chelate structure between the ($PO_4$) chains was reported by Van Wazer [9]. Glasses of $0.1Li_2O$-$0.4MO$-$0.5P_2O_5$ (M = Pb, Cu) have similar dissolution rates (Table 3). Similarly, glasses of $0.1Li_2O$-$0.4MO$-0.5P2O5 (M = Cd, Ba, Zn) have similar dissolution rates. The dissolution rate ($D_R$) of glass containing Zn or Cd is lower than that containing Pb, due to the greater binding force $Z/a^2$ of $Zn^{2+}$ and $Cd^{2+}$ ions compared to $Pb^{2+}$ ions. However, the higher $D_R$ of $0.1Li_2O$-$0.4CuO$-$0.5P_2O_5$ glass compared to $0.1Li_2O$-$0.4BaO$-$0.5P_2O_5$ glass could be explained on the basis of the dissociation energy of the M-O bond of these cations [($E_I$(Cu-O) = 343 kJ/mol) < ($E_I$(Ba-O) = 563 kJ/mol)]. The irregular change in $D_R$ with the increase in M-O bond dissociation energy suggests that there are other parameters besides density, such as the number and nature of M-O bonds, that are responsible for the change in DR. The basic structural unit of metaphosphate is the (PO3)- group, which is linked to two neighbouring phosphate groups to produce a cross-linked or chained structure. The latter is broken by the addition of network modifiers. The strength of the M-O chemical bond in glass depends on the atomic properties of the M2+ cation and, above all, on its ionic potential (charge/radius). Indeed, the energy of the Zn-O bond is greater than that of the Pb-O bond. Thus, the presence of a divalent metal Zn2+ in glass with a composition of 0.1Li2O-0.4ZnO-0.5P2O5 is expected to decrease the DR of this glass. On the contrary, the presence of $Pb^{2+}$ in $0.1Li_2O$-$0.4PbO$-$0.5P_2O_5$ glass will cause an increase in its DR. In fact, the chemical durability of lithium phosphate glasses containing ZnO is greater than that of ternary lithium and lead metaphosphate glass (Table 3). The observed improvement in durability for $0.1Li_2O$-$0.4ZnO$-$0.5P_2O_5$ glass compared to other $0.1Li_2O$-$0.4MO$-$0.5P_2O_5$ glasses (M = Cu, Cd, Ba, Pb) can be attributed to the replacement of easily hydrated P-O-P bonds by more corrosion-resistant Zn-O-P bonds when ZnO is introduced into the $Li_2O$- $P_2O_5$ glass matrix.

### 3. 4 IR spectra

Figure (3) shows the IR spectra of glasses with a composition of $0.1Li_2O$-$0.4MO$-$0.5P_2O_5$, with the frequencies and their attributions listed in Table 4.

**Table 4.** Assignment of infrared bands of glasses with composition $0.1Li_2O$-$0.4MO$-$0.5P_2O_5$

| M | Cu | Ba | Zn | Cd | Pb |
|---|---|---|---|---|---|
| δ(OPO); δ(P-O-P) | 503 | 518 | 518 | 518 | 518 |
| $\upsilon_s$(P-O-P) | 711 | 786 | 712 | 712 | 711 |
| $\upsilon_{as}$(P-O-P) | 909 | 886 | 951 | 942 | 928 |
| $\upsilon_s(PO_4^{3-})$ | 1007 | 963 | 1030 | 1016 | 951 |
| $\upsilon_{as}(PO_2^-)$ | 1072 | 1083 | 1104 | 1076 | 1044 |
| $\upsilon_s(PO_2^-)$ | 1201 | 1152 | 1230 | 1160 | 1175 |

IR spectroscopy was used to analyse the structure of $0.1Li_2O$-$0.4MO$-$0.5P_2O_5$ glasses, identifying different vibration modes:

- A vibration mode between 1080 and 1330 $cm^{-1}$ corresponds to the asymmetric stretching of the P-O-bond, while another between 1020 and 1200 $cm^{-1}$ is attributed to the symmetric stretching of this bond. The intensity and width of these modes depend on the cation present in the glass $0.1Li_2O$-$0.4MO$-$0.5P_2O_5$.
- A normal vibration mode $\upsilon_3$ of the $PO_4$ ionic group is assigned to a frequency between 940 and 1000 $cm^{-1}$.

- An asymmetric stretching vibration mode of the P-O-P bond is observed between 860–940 $cm^{-1}$, with its intensity and width varying depending on the cation in the $0.1Li_2O$-0.4MO-$0.5P_2O_5$ glass.
- A low-intensity mode at 711 $cm^{-1}$ is related to the symmetric stretching vibration of the P-O-P bridge, with a Δυ of frequencies close to 150 $cm^{-1}$, suggesting a P-O-P angle of less than 120°.
- An intense vibrational mode between 495 and 565 $cm^{-1}$ is attributed to the deformation of the P-O-P bond, with a possible contribution from $LiO_4$, and its intensity varies depending on the cation M (Cu, Cd, Zn, Ba, Pb) in the $0.1Li_2O$-0.4MO-$0.5P_2O_5$ glass.

## 3. 5 Complex impedance spectroscopies

### *3. 5. 1 Variations in complex impedance Z**

Variations in the impedance Z*=Z′+jZ″ of the electrode-electrolyte system were plotted in the complex plane (Z′, Z″) as a function of frequency. Figure (3) shows the curves for a silver/glass/silver cell as a function of temperature. In the frequency range from 20 Hz to 1 MHz, the behaviour is essentially capacitive. At temperatures above 513 K, the high-frequency experimental points lie on an arc of a circle near the origin and centred above the real axis.

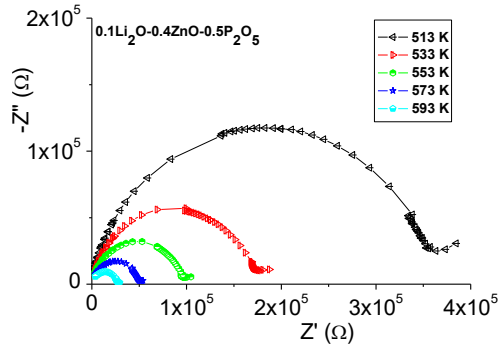


**Fig. 3.** Complex impedance plots for $0.1Li_2O$-0.4ZnO-$0.5P_2O_5$ glass at various temperatures.

### *3. 5. 2 Direct current conductivity σdc*

Conductivity measurements on $0.1Li_2O$-0.4MO-$0.5P_2O_5$ glasses were performed in a temperature range below that of the glass transition. The results show that the conductivities follow an Arrhenius law, with similar activation energies, as illustrated by the diagram $Log(\sigma_{dc})=f(10^3/T)$.

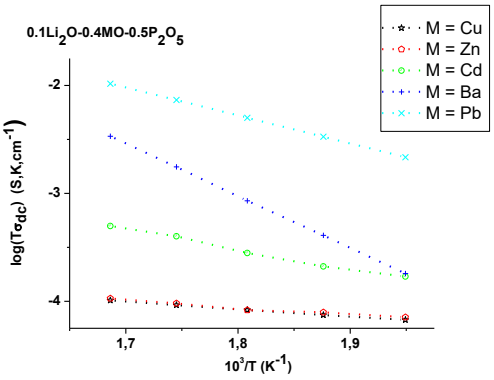


**Fig. 4.** Arrhenius diagram obtained from $0.1Li_2O$-0.4MO-$0.5P_2O_5$ glasses

In $0.1Li_2O$-0.4MO-$0.5P_2O_5$ glasses, the ionic conductivity is abnormally low for M = Cu, Cd, Zn compared to M = Pb, Ba, despite the same amount of lithium. The low ionic conductivity observed is due to the electronic conductivity in three oxide glasses containing 40 mol% of transition elements (Cu, Zn, Cd) with several valence states. The transition cations can be found in two distinct states: (x+1) and x. Conductivity does not depend linearly on the atomic number Z of divalent cations, suggesting that some lithium ions are fixed in the glass network while others, acting as network modifiers, retain their mobility. Lithium ions bound to phosphate groups are thought to be the most mobile, and their fixation may be linked to the presence of oxygen atoms not bound to phosphorus in lithium-rich glasses.

### *3. 5. 3 Alternating current conductivity σac*

Figure (5) illustrates the actual conductivity (σ') as a function of frequency at various temperatures. Conductivity is observed to be independent of frequency in a low-frequency range $\sigma_{dc}$, which becomes undetectable at low temperatures and high frequencies. At high frequencies, conductivity depends on the sample frequency σ'(ω). This behaviour of polarisation conductivity, referred to as universal dynamic response (UDR), can be expressed by a simple relationship: $\sigma_{ac} = \sigma_{dc}+\sigma'(\omega)$ (Eq. 4).

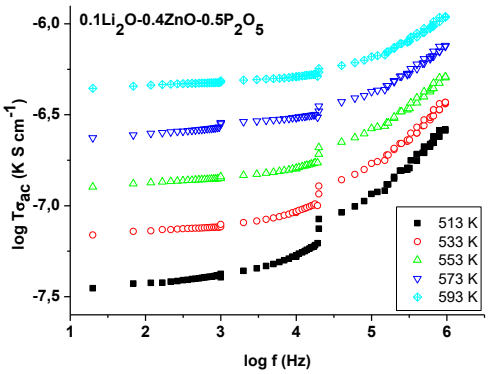


**Fig. 5.** Alternating current conductivity $\sigma_{ac}$ of $0.1Li_2O$-$0.4ZnO$-$0.5P_2O_5$ glass at different temperatures in a frequency range of 20 Hz to 1 MHz.

The values of conductivity $\sigma_{dc}$, frequencies $f_0$ and $f_{pol}$ are evaluated using the $\sigma_{ac}$ curve according to log f. The results show that $\sigma_{dc}$ increases in the following order: $\sigma_{dc}(Cd) < \sigma_{dc}(Cu) < \sigma_{dc}(Zn) < \sigma_{dc}(Ba) < \sigma_{dc}(Pb)$. Conductivity $\sigma_{ac}$ is observed to be frequency-dependent, highlighting dispersive behaviour attributed to electrode polarisation.

### *3. 5. 4 Dielectric relaxations: frequency response*

This study determines the parameters of charge carriers, such as the hopping frequency $f_p$ and relaxation time $\tau_\sigma$, using the complex modulus formalism, $M^* = 1/\varepsilon^* = j\omega C0Z^*$. This formalism avoids problems related to electrode polarisation and interfacial effects in solid electrolytes. The variation of log (M′) as a function of log f at different temperatures is illustrated for the $0.1Li_2O$-$0.4CuO$-$0.5P_2O_5$ glass (Figure (6-a)), showing that (M′) reaches a constant value at high frequency and low temperature, thus confirming the negligible polarisation of the electrodes in the temperature range studied.
The normalised imaginary part $M''/M''_{max}$ of the $0.1Li_2O$-$0.4ZnO$-$0.5P_2O_5$ glass is shown at different temperatures in Figure (6-b).

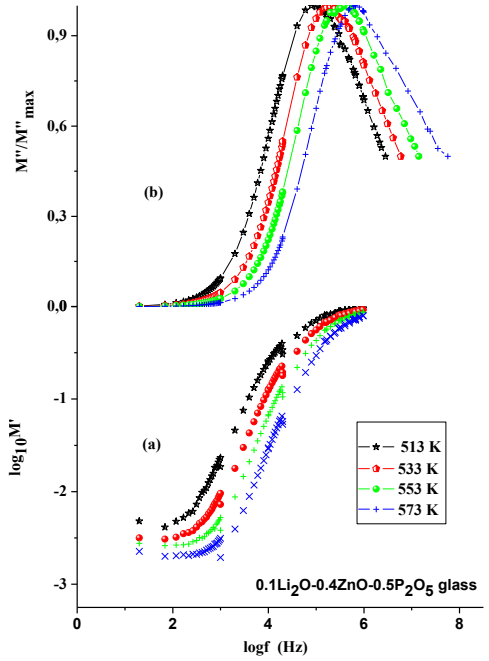


**Fig. 6.** Electrical modulus M′ (a) and $M''/M''_{max}$ (b) of $0.1Li_2O$-$0.4ZnO$-$0.5P_2O_5$ glass at different temperatures.

At a given temperature, the spectra show asymmetric peaks centred around M*. The maximum of M″ corresponds to a characteristic frequency fp. To the left of the peak, long-distance movements of mobile ions are observed, while to the right, the ions are more confined in their potential wells. The frequency range of the peak indicates a shift from short-distance mobility to long-distance mobility [10]. The relationship $\omega\tau_\sigma = 1$ quantitatively characterises the conductivity relaxation time $\tau_\sigma$ [11]. With increasing temperature, the asymmetric peaks of M″ shift towards higher frequencies [12], indicating non-exponential conductivity relaxation behaviour. The peak width exceeds that associated with Debye behaviour [13]. For $0.1Li_2O$-$0.4MO$-$0.5P_2O_5$ glasses, the β value of the Kohlrausch parameter increases in the order $\beta(Cd) < \beta(Cu) < \beta(Zn)$, and the variation in frequency $f_p$, defined by $f_p = 1/2\ \tau_\sigma$ and normalised with respect to $M''_{max}$, is illustrated in Figure (7).

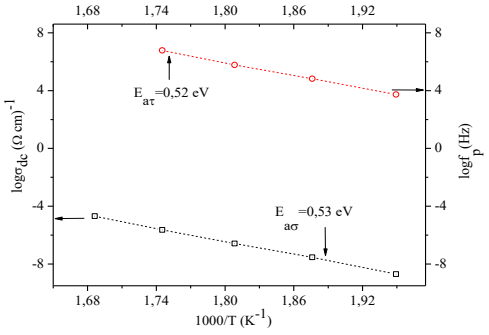

**Fig. 7.** Variation in conductivity log($\sigma_{dc}$) and relaxation frequency log($f_p$) of $0.1Li_2O$-$0.4MO$-$0.5P_2O_5$ glass with temperature.

An Arrhenius-type law is observed for conductivity $\sigma_{dc}$ as a function of temperature, with quasi-parallel straight lines suggesting similar activation energies $E_{a\sigma}$ and $E_{a\tau}$, listed in Table (5). This indicates that ion transport in $0.1Li_2O$-$0.4MO$-$0.5P_2O_5$ glasses results from a "hopping" mechanism [14].

**Table 5**. SIC data for $0.1Li_2O$-$0.4MO$-$0.5P_2O_5$ glasses.

| M | $\log\sigma_{dc}$ à 300K (S cm$^{-1}$) | $\text{Log}\sigma_0$ (S cm$^{-1}$) | $\log\tau_0\times10^2$ | $E_{a\sigma}$ (eV) | $E_{a\tau}$ (eV) | s | β |
|---|---|---|---|---|---|---|---|
| Cd | -14.96 | 5.67 | 0.84 | 0.68 | 0.67 | 0.51 | 0.63 |
| Cu | -14.60 | 5.31 | 0.86 | 0.61 | 0.60 | 0.53 | 0.65 |
| Zn | -13.20 | 4.64 | 0.95 | 0.54 | 0.53 | 0.54 | 0.68 |
| Ba | -11.36 | 3.12 | 1.24 | 0.43 | 0.43 | - | - |
| Pb | -10.09 | 2.73 | 1.42 | 0.38 | 0.37 | - | - |

The values of the β parameter derived from the $M''/M''_{max}$ curves are less than 1, suggesting a relaxation time distribution in the $0.1Li_2O$-$0.4MO$-$0.5P_2O_5$ glasses. This interpretation is common for various solid electrolytes [15], However, recent studies [16] challenge this hypothesis. Using this methodology on $0.1Li_2O$-$0.4CuO$-$0.5P_2O_5$ glass, several frequency-dependent curves were obtained, including log($\sigma_{ac}/\sigma_{dc}$)(c), log M′ (a) and $M''/M''_{max}$ (b) (Figure 8).

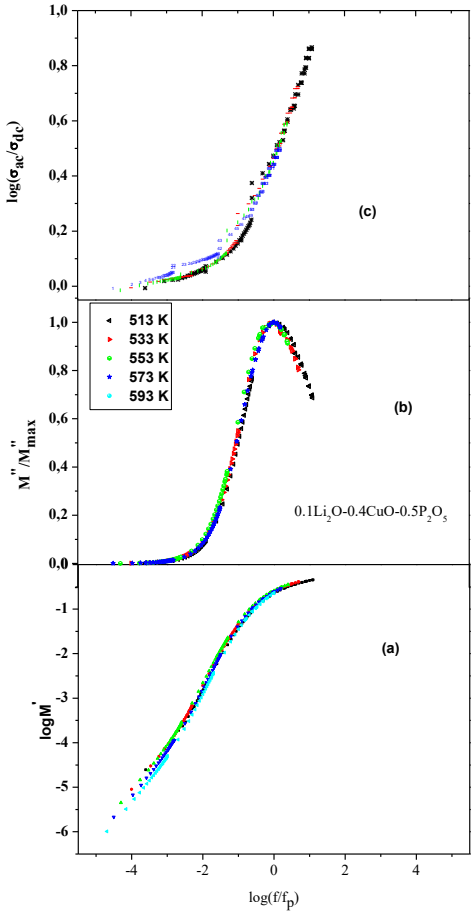


**Fig. 8.** The 'parent' curves (log($\sigma_{ac}/\sigma_{dc}$) (c), logM′ (a), $M''/M''_{max}$ (b)) as a function of the normalised frequency log($f/f_p$) of $0.1Li_2O$-$0.4CuO$-$0.5P_2O_5$ glass at different temperatures.

The curves in Figures 8a, 8b, and 8c show that electrical elements at different frequencies exhibit similar variations depending on temperature, indicating uniform activation energy [17]. This

contradicts the hypothesis of a relaxation time distribution to explain the non-exponential relaxation of conductivity in the glasses examined, suggesting that the dynamic processes are independent of temperature and that the conduction mechanism remains constant.

The diffractograms of the glasses studied show a completely amorphous structure, with no significant crystalline peaks, confirming their amorphous nature. On the other hand, glasses annealed at temperatures below their melting point recrystallise, forming the crystalline phase $LiPb_2(PO_3)_5$ for the glass $0.1Li_2O$-$0.4PbO$-$0.5P_2O_5$ (Figure 9).

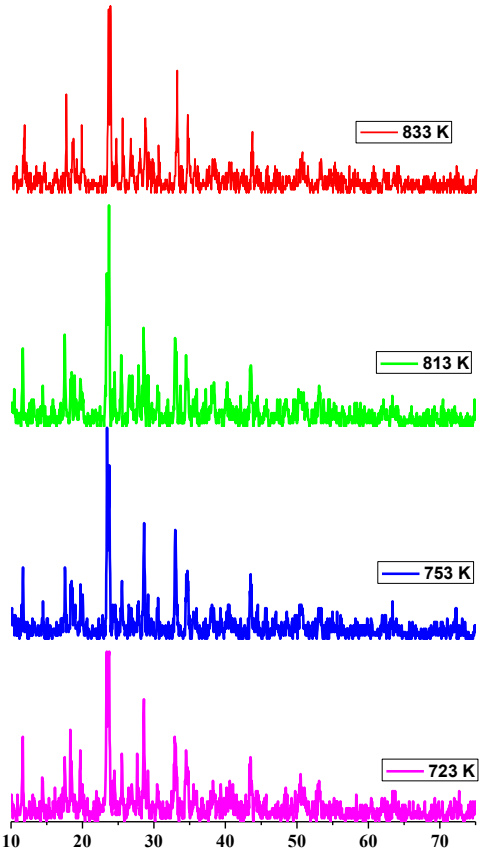


**Fig. 9.** Diffractograms obtained at different temperatures for $0.1Li_2O$-$0.4PbO$-$0.5P_2O_5$ glass

**Table 6.** Crystallographic data for $LiPb_2(PO_3)_5$

| | |
|---|---|
| Formula | $LiPb_2(PO_3)_5$ |
| Molar mass | M = 816.20 g $mol^{-1}$ |
| Crystalline system | Monoclinic |
| Space group | P2/n (No. 13) |

## 3. 6 Devitrification of $0.1Li_2O$-$0.4MO$-$0.5P_2O_5$ glasses

| | |
|---|---|
| Mesh settings | a =12.28 Å; b=9.689 Å; c=5.523Å; β = 91.01 |
| Mesh volume | V = 657.51 $Å^3$ |
| Form groups | Z = 8 |
| Calculated density | $D_c$ = 4.123 g $cm^{-3}$ |
| ID | 78-0332 |
| ICSD | 061207 |

The elementary mesh has two centrosymmetric chains $(PO_3)_\infty$ that extend parallel to dimension c. Each chain consists of five tetrahedra, three of which are independent with two axes 2 located at x = ¼, z = ¼ and x = ¼, z = ¼ (Fig. 10).

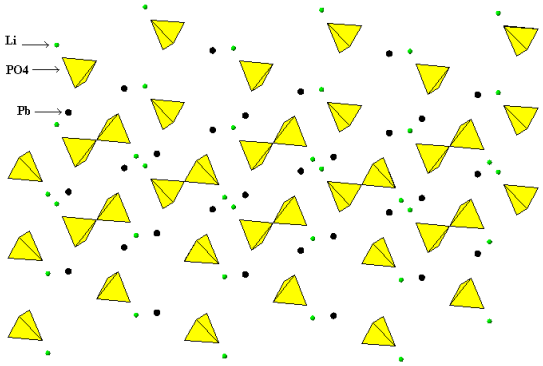


**Fig. 10.** Projection of the $LiPb_2(PO_3)_5$ structure along the b axis onto the ac plane, highlighting highly curved $(PO_3)_x$ chains.

Lead is surrounded by seven oxygen atoms, with distances ranging from 2.45 to 2.93 Å. This same environment is observed in other phosphates, such as the mixed lead and potassium polyphosphate $PbK_2(PO_3)_4$ [18]. $PbO_7$ lead polyhedral are linked parallel to the diagonal (a + c), sharing an edge. The smallest Pb-Pb distance is 4.218 Å.

Due to its position relative to the centre of symmetry, lithium has only five oxygen neighbours, forming a pseudo-quadratic pyramid-shaped $LiO_5$ polyhedron. The Li-O distance varies from 1.973 to 2.439 Å, with specific coordination observed in $Cu_2Li_2P_6O_{18}$ [19]. $LiO_5$ pyramids are isolated by chains of $PO_4$ tetrahedra and $PbO_7$ polyhedral, connected by centre symmetry via a common face and edge.

The cation can behave in two ways at this site: either it distributes itself statistically with an occupancy rate of 0.5 between two centre-symmetric positions 0.96 Å apart, or it moves rapidly between these positions around the central plane of the bipyramid.

## Conclusion

This work determined the density, glass transition temperature, chemical durability and electrical properties of $0.1Li_2O$-$0.4MO$-$0.5P_2O_5$ glasses, studying their dependencies on the incorporation of the divalent cation into the $Li_2O$-$P_2O_5$ glass matrix.

- The molar volume of the glasses studied follows the order: $V_m(Cu) < V_m(Zn) < V_m(Cd) < V_m(Pb) < V_m(Ba)$, in relation to the increase in the atomic molecular weight of the divalent cation with M (Cu, Cd, Zn, Ba, Pb).
- The dissolution rate of metals follows the order $D_R(Zn) < D_R(Cd) < D_R(Ba) < D_R(Cu) < D_R(Pb)$, due to the density of the glass and the nature and strength of the M-O bond.
- The increase in glass transition temperature ($T_g$) follows the order $T_g(Pb) < T_g(Cd) < T_g(Ba) < T_g(Zn) < T_g(Cu)$ and can be interpreted as a deconvolution of the increase in compactness ($V_t$).
- The structure of the lithium phosphate matrix is modified by the cation M (Cu, Cd, Zn, Ba, Pb) in the glass $0.1Li_2O$-$0.4MO$-$0.5P_2O_5$, resulting in variations in the intensity and width of the IR vibration modes with the addition of MO, considered as an intermediate.
- The conductivity σdc, relaxation time, activation energies $E_{a\sigma}$, $E_{a\tau}$, $\sigma_0$, and $f_0$ of $0.1Li_2O$-$0.4MO$-$0.5P_2O_5$ glasses vary depending on the divalent metal cation M studied (Cu, Cd, Ba, Pb, Zn). Glasses containing M (Ba, Pb) exhibit better performance (higher $\sigma_{dc}$ and $\tau_\sigma$, and lower activation energy values) than those with M (Zn, Cu, Cd), due to greater Li ion mobility resulting from higher molar volume. Furthermore, these two glasses (Pb, Ba) have negligible electronic conductivity.
- The activation energies $E_{a\sigma}$ and $E_{a\tau}$, being very close, indicate that ion transport in $0.1Li_2O$-$0.4MO$-$0.5P_2O_5$ glasses results from a " hopping " mechanism».
- The evolution of M′ as a function of frequency at different temperatures for $0.1Li_2O$-$0.4MO$-$0.5P_2O_5$ glasses indicates that, at high frequency and low temperature, the M′ values converge towards constant levels, confirming that electrode polarisation is negligible.
- The overlap of the 'parent' curves ($\log(\sigma_{ac}/\sigma_{dc})$, logM′ and $M''/M''_{max}$) indicates that the dynamic processes are independent of temperature and that the conduction mechanism remains unchanged for the glasses studied.

The study concludes various insights regarding the recrystallization of glasses from the ternary system $0.1Li_2O$-$0.4MO$-$0.5P_2O_5$, where M can be Cu, Cd, Zn, Ba, or Pb. The devitrification of $0.1Li_2O$-$0.4PbO$-$0.5P_2O_5$ glass has led to the identification of a new material, $LiPb_2(PO_3)_5$, which crystallises in the monoclinic system. It appears that the Li cation does not occupy a symmetrical octahedral site due to significant thermal agitation. Neutron diffraction could help confirm the position of lithium outside the centre of symmetry, although it is not sufficient to characterise the type of disorder present.

## References

[1] Brow RK., La structure des verres de phosphate simples, J. Non-cryst. Solids, 263 (2000) 1-28. https://doi.org/10.1016/S0022-3093(99)00620-1.

[2] Muruganandam K., Seshasayee M., & Patnaik S., An X-ray RDF study of $Li_2O$- $P_2O_5$-LiCl glasses. Solid State Ion., 89(3-4) (1996) 313-319. https://doi.org/10.1016/S0022-3093(99)00620-1.

[3] Ahmina W., El Moudane M., Zriouil M., & Taibi MH., Région de formation de verre, structure et quelques propriétés des verres de phosphate de potassium et de manganèse, Ph. Transit., 89 (11) (2016) 1051-1061. https://doi.org/10.1080/01411594.2016.1144057.

[4] El Hezzat M., Et-Tabirou M., Montagne L., Palavit G., Mazzah A., & Dhamelincourt P., Études spectroscopiques de la structure des verres métaphosphates $Na_2O$-CdO-PbO-$P_2O_5$. Phys. Chem. Glasses, 44 (5) (2003) 345-348.

[5] Muñoz F., Rocherullé J., Ahmed I., & Hu L. (2019). Phosphate glasses. In Springer handbook of glass (pp. 553-594). Cham: Springer International Publishing.

[6] Nzaba Madila E. E. (2022). Synthèse et caractérisation de phosphates de métaux de transition de type Na2+ 2xCo8-yMz (PO4) 6 comme composants pour batteries ions sodium (Doctoral dissertation, Université du Québec à Trois-Rivières).

[7] Ellmer K., Klein A., & Rech B. (Eds.). (2007). Oxyde de zinc conducteur transparent: principes de base et applications dans les cellules solaires à couches minces.

[8] Ray NH., Relations composition-propriété dans les verres d'oxyde inorganiques. J. Non -cryst. Solids, 15 (3) (1974) 423-434. https://doi.org/10.1016/0022-3093(74)90148-3.

[9] Wazer JRV., Structure et propriétés des phosphates condensés. II. Une théorie de la structure moléculaire des verres de phosphate de sodium1, J. Am. Chem. Soc., 72 (2) (1950) 644-647. https://doi.org/10.1021/ja01158a002.

[10] Howell F. S., Bose R. A., Macedo P. B., & Moynihan C. T., Electrical relaxation in a glass-forming molten salt, J. Phys. Chem., 78(6) (1974) 639-648. https://doi.org/10.1021/j100599a016.

[11] Patel HK et Martin SW. Conduction ionique rapide dans les verres Na 2 S+ B 2 S 3:

contributions compositionnelles à la non-exponentielle de la relaxation de la conductivité dans la limite des métaux alcalins extrêmement faibles. Physical Review B, ***45 (18)*** (1992) 10292. DOI: https://doi.org/10.1103/PhysRevB.45.10292.

[12] Ngai KL, & Martin SW., Corrélation entre l'enthalpie d'activation et l'exposant de Kohlrausch pour la conductivité ionique dans les verres d'oxyde. Physical Review B, ***40*** (15) (1989) 10550. DOI: https://doi.org/10.1103/PhysRevB.40.10550.

[13] Zouari N., Mnif M., Khemakhem H., Mhiri T., & Daoud A., Paramètres de relaxation de la conductivité de certains $H^+$ et $K^+$ conducteurs dans le composé polycristallin $KD_yHP_3O_{10}$. Solid State Ionics, 110 (3-4) (1998) 269-275. https://doi.org/10.1016/S0167-2738(98)00128-3.

[14] Chowdari BVR., and Radhakrishnan K., Caractérisation électrique et électrochimique d'électrolytes solides à base de $Li_2O$- $P_2O_5$-$Nb_2O_5$, J. Non-cryst. Solids, 110 (1) (1989) 101-110. https://doi.org/10.1016/0022-3093(89)90187-7.

[15] Kawamura J., & Shimoji M., Transition vitreuse et conductivité AC des verres conducteurs $Ag^+$. Chimie et physique des matériaux, 23 (1-2) (1989) 99-120. https://doi.org/10.1016/0254-0584(89)90020-5.

[16] Jain, SC, & Hayes, W., Structure, propriétés et applications des couches contraintes et des superréseaux GexSi1-x. Semi-conductor, SciTech, 6 (7) (1991) 547-576. DOI 10.1088/0268-1242/6/7/001.

[17] Ngai KL., & Roland CM., Structure chimique et coopérativité intermoléculaire: résultats de relaxation diélectrique, Macromolécules, 26 (25) (1993) 6824-6830. https://doi.org/10.1021/ma00077a019.

[18] El-Horr N., & Bagieu-Beucher M., Structure d'un polyphosphate mixte de plomb et de lithium, $Pb_2Li(PO_3)_5$. Acta Crystallogr., Sect. C: Cryst. Struct. Commun, 42(6) (1986) 647-651. https://doi.org/10.1107/S0108270186095057.

[19] Laügt M., & Durif A., Structure cristalline de l'hexamétaphosphate de cuivre-lithium, $Cu_2Li_2P_6O_{18}$, Structural Science, 30(9) (1974) 2118-2121. https://doi.org/10.1107/S0567740874006571

.